Field-Free Three Dimensional Molecular Axis Alignment

Jonathan G. Underwood,[1,*] Benjamin J. Sussman,[2,3] and Albert Stolow[2,3]

[1]*Department of Physics and Astronomy, The Open University, Walton Hall, Milton Keynes, United Kingdom, MK7 6AA*

[2]*Steacie Institute for Molecular Sciences, National Research Council of Canada, 100 Sussex Drive, Ottawa, Ontario, K1A 0R6, Canada*

[3]*Department of Physics, Queen's University, Kingston, Ontario, K7L 3N6, Canada*

(Received 28 May 2004; published 13 April 2005)

We investigate strategies for field-free three dimensional molecular axis alignment using strong nonresonant laser fields under experimentally realistic conditions. Using the polarizabilites and rotational constants of an asymmetric top rotor molecule (ethene, C_2H_4), we consider three different methods for axis alignment of a Boltzmann distribution of rotors at 4 K. Specifically, we compare the use of impulsive kick laser pulses having both linear and elliptical polarization to the use of elliptically polarized switched laser pulses. We show that an enhanced degree of field-free three dimensional alignment of ground vibronic state molecules obtains from the use of two orthogonally polarized, time-separated laser pulses.

DOI: 10.1103/PhysRevLett.94.143002 PACS numbers: 33.15.Kr, 33.15.Mt, 33.80.Wz

As electric forces govern much of molecular and solid state physics, the ability to precisely apply strong fields to material systems is one of the principal tools of femtosecond laser science. One important example of this electrical manipulation is given by molecular alignment in strong nonresonant laser fields [1,2]. Molecular axis alignment can bring the molecular frame, where molecular processes occur, into the lab frame where measurements are made. This benefits emerging techniques for the study of molecular structure and dynamics wherein orientational averaging of the molecular frame leads to considerable loss of information. Examples include time-resolved photoelectron spectroscopy [3–5], time-resolved x-ray [6–8] and electron diffraction [9,10], timed Coulomb explosion [11,12], and most recently, high-order harmonic generation [13]. However, in order to probe native structure and dynamics, the measurements must be made field free, i.e., in the absence of the alignment field that would otherwise strongly perturb the system. Furthermore, polyatomic molecules have a three dimensional structure, requiring alignment of all three molecular axes. Three dimensional alignment in the presence of a strong elliptically polarized laser field has been demonstrated [14]. In the following, we present our studies of field-free three dimensional molecular axis alignment (FF3DA) of asymmetric top polyatomic molecules.

Single axis (one dimensional) field-free alignment was demonstrated for linear [15–17] and asymmetric top molecules [18] using short impulsive (''kick'') pulses [19–21] which nonadiabatically create rotational wave packets. Recently, one dimensional alignment has also been achieved using a sequence of two time delayed laser pulses [22,23]. The sudden truncation of an adiabatically applied strong field, generating ''switched'' rotational wave packets, also creates field-free one dimensional alignment [24]. These results led to proposals that FF3DA may be achievable either by (i) an elliptically polarized impulsive kick laser pulse [18] or by (ii) an elliptically polarized field which turns on adiabatically and is truncated rapidly [24]. Here we show that a more successful method of producing FF3DA is to use two time separated, linearly polarized laser pulses having orthogonal polarization directions. The initial laser pulse kicks the most polarizable molecular axis towards alignment with the laser polarization vector, creating a rotational wave packet. Subsequent revivals of this wave packet will exhibit single dimensional alignment of one molecular axis, while maintaining cylindrical symmetry and confining the remaining two axes towards the plane perpendicular to the laser polarization vector. Application of a second laser pulse linearly polarized orthogonally to the first and temporally coincident with a revival of this wave packet will kick the most polarizable of the remaining two axes towards alignment with the second laser polarization, breaking the cylindrical symmetry of the system. The subsequent wave-packet evolution exhibits FF3DA.

To proceed, we require a description of the alignment of an asymmetric top molecule with multiple nonresonant laser fields, allowing for noncoincident polarizations and/or propagation directions. In order to provide a realistic assessment of these schemes in experimentally realistic conditions, we present calculations of the degree of FF3DA for the representative asymmetric top molecule ethene where we have included the full distribution of thermally populated initial rotational energy levels. The calculations presented here are for ethene gas at a rotational temperature of 4 K, typical of the conditions achievable in gas phase molecular beam experiments. The interaction of a ground vibronic state molecule with a number of strong nonresonant laser fields of the form $\mathbf{E}(t) = \sum_i \mathcal{E}_i(t)\hat{\mathbf{e}}_i \cos(\omega_i t)$, where $\mathcal{E}_i(t)$ is the pulse envelope and $\hat{\mathbf{e}}_i$ is the polarization vector of the laser field of carrier frequency ω_i, in the limit of a dominating Raman type interaction may be described by an effective Hamiltonian [24,25] decomposed into spherical tensor form [26]

$$V(t) = -\sum_{ij} \mathcal{E}_i^*(t)\mathcal{E}_j(t)\sum_{kp}(-1)^{k-p}[\hat{\mathbf{e}}_i^* \otimes \hat{\mathbf{e}}_j]_p^k \alpha_{-p}^k. \quad (1)$$

Here α_{-p}^k are the spherical tensor components of the molecular polarizability tensor in the laboratory frame (LF) and $[\hat{\mathbf{e}}_i^* \otimes \hat{\mathbf{e}}_j]_p^k$ are the spherical tensor components of the polarization tensor describing the electric fields of the laser pulses in the LF. The polarization tensor depends upon the experimental geometry only (i.e., the polarizations and propagation directions of the lasers) and is readily calculated by extension of the formalism of Kummel *et al.* [27] to multiple laser fields. The LF components of the polarizability tensor α_p^k are related to the molecular frame (MF) components through the rotation $\alpha_p^k = \sum_q D_{pq}^{k*}(\phi, \theta, \chi)\alpha_q^k$, where (ϕ, θ, χ) are the Euler angles connecting the LF and MF and $D_{pq}^{k*}(\phi, \theta, \chi)$ is a Wigner rotation matrix [26]. These equations allow for the separation of the MF properties from the LF properties. In the absence of a resonance, only MF polarizability tensor components with $k = 0, 2$ are nonzero. Furthermore, only even q components are nonzero and are given in terms of the real Cartesian components by $\alpha_0^0 = -\frac{1}{\sqrt{3}} \times (\alpha_{xx} + \alpha_{yy} + \alpha_{zz})$, $\alpha_0^2 = \frac{1}{\sqrt{6}}(2\alpha_{zz} - \alpha_{yy} - \alpha_{zz})$, and $\alpha_{\pm 2}^2 = \frac{1}{2}(\alpha_{xx} - \alpha_{yy})$. Here and in the discussion that follows, we use (x, y, z) to refer to the Cartesian axes in the MF, and (X, Y, Z) to refer to the Cartesian axes in the LF.

The field-free rigid rotor Hamiltonian of an asymmetric top molecule is written as $H_0 = B_x\mathbf{J}_x^2 + B_y\mathbf{J}_y^2 + B_z\mathbf{J}_z^2$, where B_x, B_y, and B_z are the rotational constants of the molecule. The wave function may be expressed as a superposition of the eigenstates of this Hamiltonian, $\Psi(t) = \sum_{JMn} C_{JMn}(t)e^{-iE_{Jn}t/\hbar}|JMn\rangle$, where J and M are the quantum numbers for the angular momentum and its projection upon the LF Z axis, respectively, and n labels the $(2J + 1)$ eigenstates with the same values of (J, M). Substituting this wave function into the time-dependent Schrödinger gives the following equation of motion for the $C_{JMn}(t)$ coefficients

$$i\hbar\dot{C}_{JMn}(t) = \sum_{J'M'n'} C_{J'M'n'}(t)e^{i(E_{Jn}-E_{J'n'})t/\hbar} \times \langle JMn|V(t)|J'M'n'\rangle. \quad (2)$$

Expanding the asymmetric top eigenstates in the symmetric top basis [26] gives

$$\langle JMn|V(t)|J'M'n'\rangle = (2J+1)^{1/2}(2J'+1)^{1/2}\sum_{ij}\mathcal{E}_i^*(t)\mathcal{E}_j(t) \times \sum_{KK'} a_K^{Jn} a_{K'}^{J'n'}(-1)^{M'-K'} \times \sum_k (-1)^{k-q}[\hat{\mathbf{e}}_i^{1*} \otimes \hat{\mathbf{e}}_j^1]_p^k \alpha_{-q}^k \times \begin{pmatrix} J & k & J' \\ M & p & -M' \end{pmatrix}\begin{pmatrix} J & k & J' \\ K & q & -K' \end{pmatrix}, \quad (3)$$

where a_K^{Jn} are the symmetric top basis eigenvector coefficients with K the quantum number for the projection of J upon the MF z axis. From the properties of the Wigner 3-j symbol, nonzero matrix elements have $p = M' - M = 0, \pm 1, \pm 2$, $q = K' - K = 0, \pm 2$, $k = 0, 2$, and $J' = J, J \pm 1, J \pm 2$.

To characterize the induced alignment we calculate the expectation values of the squared direction cosine matrix elements connecting the LF and MF, $\langle\Phi_{Fg}^2\rangle$, with $F \in \{X, Y, Z\}$ and $g \in \{x, y, z\}$ and $\Phi_{Fg} = \hat{\mathbf{F}} \cdot \hat{\mathbf{g}}$ [26]. The value of $\langle\Phi_{Fg}^2\rangle$ reflects the correlation between the LF F axis and MF g axis, taking a value between 0 for maximal antialignment and 1 for maximal alignment. An isotropic ensemble will have all $\langle\Phi_{Fg}^2\rangle = \frac{1}{3}$. These expectation values are averaged over the Boltzmann distribution of initial energy level populations. Following spectroscopic convention, we associate the MF coordinates with the principal axes (a, b, c) for ethene as $z = a$, $x = b$, and $y = c$. The a axis lies along the C = C bond, the b axis lies perpendicular to the plane of the molecule, and the c axis lies perpendicular to the C = C bond in the plane of the molecule. The principal axes a, b, and c have associated rotational constants $A = 4.828\ \text{cm}^{-1}$, $B = 1.001\ \text{cm}^{-1}$, and $C = 0.828\ \text{cm}^{-1}$, respectively. The three polarizability components were taken to be $\alpha_{aa} = 1.692\ \text{Å}^3$, $\alpha_{bb} = 1.066\ \text{Å}^3$, and $\alpha_{cc} = 1.491\ \text{Å}^3$. In general, the choice of the principal axes for the molecule will depend upon the type and symmetry of the molecule [26]. We take all laser pulse envelopes to be of the form $\mathcal{E}(t) = \mathcal{E}_0 e^{-(t-t_0)^2/2T^2}$, where $T = \tau_{\text{rise}}$ for $t < t_0$ and $T = \tau_{\text{fall}}$ for $t > t_0$ and $\mathcal{E}_0$ is the peak laser electric field at t_0.

In Fig. 1 we show the alignment produced by a single linearly polarized kick pulse for a laser peak intensity of $10^{12}\ \text{W/cm}^2$. Plotted here are the three expectation values, $\langle\Phi_{Xb}^2\rangle$, $\langle\Phi_{Yc}^2\rangle$, and $\langle\Phi_{Za}^2\rangle$. The most polarizable MF axis, a, is kicked towards alignment along the polarization direction causing revivals in $\langle\Phi_{Za}^2\rangle$ and strong alignment of a along Z after the laser pulse. Commensurate with the revival structure in $\langle\Phi_{Za}^2\rangle$ are peaks in $\langle\Phi_{Xb}^2\rangle$ and $\langle\Phi_{Yc}^2\rangle$ as is expected classically; localizing the a axis along Z results in a localization of the b and c axes towards the X-Y plane. However, unconstrained rotation about a results in there being no three dimensional alignment; the calculation shows that at all times $\langle\Phi_{Xb}^2\rangle = \langle\Phi_{Yb}^2\rangle$ and $\langle\Phi_{Yc}^2\rangle = \langle\Phi_{Xc}^2\rangle$; i.e., there is no localization of b or c along either X or Y and the alignment is one dimensional. The revival structure in $\langle\Phi_{Za}^2\rangle$ arises due to J-type coherences between states with $|\Delta J| = 1, 2$ giving rise to frequency components spaced by $2(B + C)$. Additionally, the asymmetry of the molecule introduces frequency components spaced by $4C$ caused by coherences between states with $|\Delta J| = 2$ [28]. The faster modulation seen in $\langle\Phi_{Xb}^2\rangle$ and $\langle\Phi_{Yc}^2\rangle$, due to rotation about the low moment of inertia a axis, contains frequency components spaced by $4A$ from coherences between states with $|\Delta J| = 2$, and components spaced by

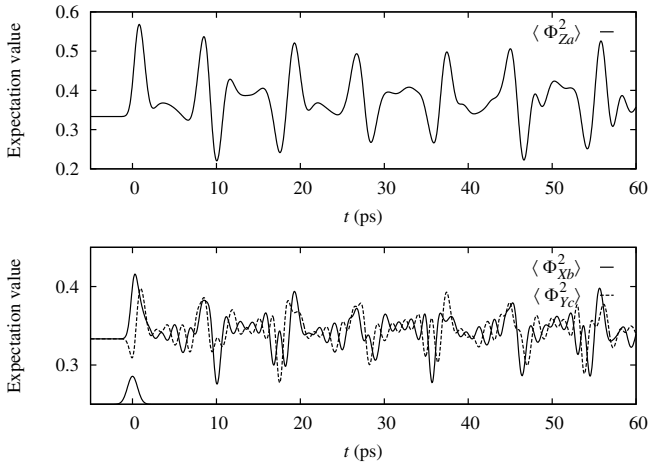

FIG. 1. Alignment of ethene at a rotational temperature of 4 K with a linearly polarized kick pulse with $\tau_{\text{rise}} = \tau_{\text{fall}} = 600$ fs, $t_0 = 0.0$ ps, and $\mathcal{E}_0 = 2.746 \times 10^9$ (corresponding to 10^{12} W/cm^2) polarized along the LF Z axis. The pulse envelope is indicated below the lower plot.

$4A - (2B + C)$ caused by K-type coherences between states with $\Delta J = 0$. These coherences of spacing Δf have associated recurrences at $t = n/\Delta f$ where n is an integer. In Fig. 2 we consider the application of a second perpendicular polarized kick pulse at a time coincident with a revival of the wave packet when $\langle \Phi^2_{Za} \rangle$ is maximal. This second laser pulse is polarized along the X axis and is chosen to be significantly shorter than the duration of the revival associated with $\langle \Phi^2_{Za} \rangle$. During the period when $\langle \Phi^2_{Za} \rangle$ is maximal, the orthogonally polarized second laser pulse exerts minimal torque upon the a axis while inducing rotation about the a axis to bring c into alignment with X. A shorter second laser pulse is advantageous in this case because rotation about a is more rapid than rotation about b and c due to the lower moment of inertia. As can be seen from examining both $\langle \Phi^2_{Xc} \rangle$ and $\langle \Phi^2_{Xc} \rangle - \langle \Phi^2_{Yc} \rangle$ in Fig. 2, this second laser pulse induces subsequent strong field-free alignment of the c axis with the X axis at times coincident with strong alignment of the a axis with the Z axis when compared to the situation with just the single initial Z polarized laser pulse. The associated degree of FF3DA for the two laser pulse case is optimal with $\langle \Phi^2_{Xc} \rangle$ taking values equal to $\langle \Phi^2_{Za} \rangle$ at some times. For example, at 44.9 ps, $\langle \Phi^2_{Za} \rangle = \langle \Phi^2_{Xc} \rangle = 0.5$. By using higher laser intensities, it would be possible to further increase the degree of FF3DA (subject to keeping the intensity low enough to avoid ionization).

For comparison, we consider the previously suggested application of elliptically polarized kick [18] and switched [24] pulses to the creation of FF3DA. In Figs. 3 and 4 we examine the degree of three dimensional alignment with elliptically polarized laser fields propagating along the LF Y axis, with the major axis of the polarization ellipse along the Z axis and the minor axis along the X axis. In an elliptically polarized laser field, it is expected that the most polarizable molecular axis, in this case a, will become aligned along the major axis of the polarization ellipse, Z, while the next most polarizable molecular axis, in this case c, will become aligned along the minor axis of the ellipse, X [14]. In Fig. 3 we examine the effect of an elliptically polarized switched laser pulse which turns

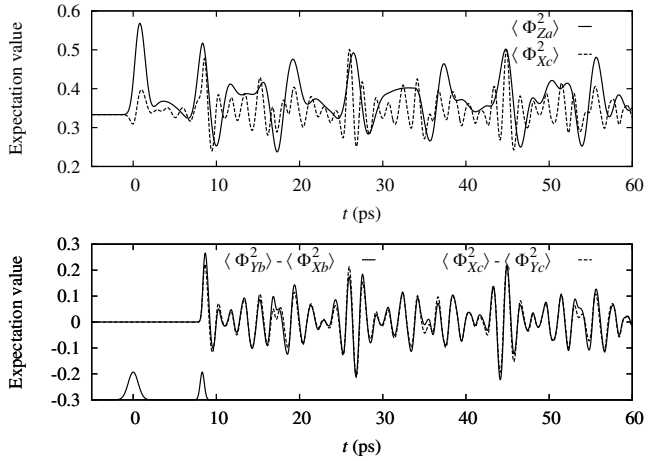

FIG. 2. Alignment of ethene at a rotational temperature of 4 K with two linearly polarized kick laser pulses propagating along the LF Y axis. The first laser pulse at $t_0 = 0.0$ ps is linearly polarized along Z with $\tau_{\text{rise}} = \tau_{\text{fall}} = 600$ fs. The second laser pulse at $t_0 = 8.3$ ps is linearly polarized along X with $\tau_{\text{rise}} = \tau_{\text{fall}} = 250$ fs. Both laser pulses have a peak electric field of $\mathcal{E}_0 = 2.746 \times 10^9$ V/m. The pulse envelopes are indicated below the lower plot.

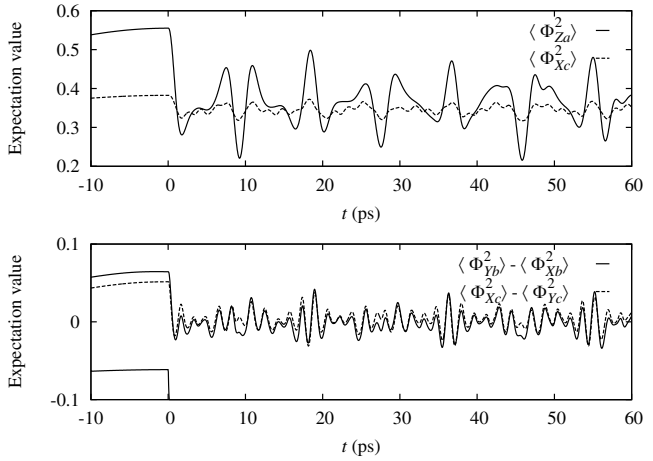

FIG. 3. Alignment of ethene at a rotational temperature of 4 K with an elliptically polarized switched laser pulse propagating along the LF Y axis with $\tau_{\text{rise}} = 30$ ps, $\tau_{\text{fall}} = 50$ fs, and $t_0 = 0$ ps. A peak laser field of $\mathcal{E}_0 = 2.972 \times 10^9$ V/m was used with the major axis of the polarization ellipse along the Z axis and a phase difference of $\pi/8$ between the Z and X components (i.e., $e_Z = 0.924$ and $e_X = -0.383i$). The pulse envelope is indicated below the lower plot.

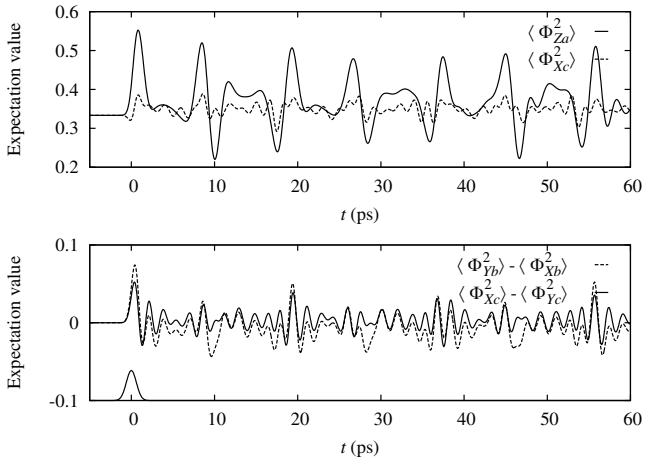

FIG. 4. Alignment of ethene at a rotational temperature of 4 K with an elliptically polarized kick pulse propagating along the LF Y axis with $\tau_{\text{rise}} = \tau_{\text{fall}} = 600$ fs and $t_0 = 0.0$ ps. The polarization vector components and peak electric field were chosen to be the same as for Fig. 3. The pulse envelope is indicated below the lower plot.

on adiabatically (i.e., much slower than molecular rotation) and truncates rapidly, suddenly projecting the adiabatically prepared state back onto the field-free eigensystem [24] and in Fig. 4 we consider the effect of an elliptically polarized kick pulse with the same peak intensity and polarization state. Comparison of $\langle \Phi^2_{Xc} \rangle$ (and $\langle \Phi^2_{Yb} \rangle$, not shown) with $\langle \Phi^2_{Za} \rangle$ in these figures shows that the degree of alignment of c with X, and b with Y is significantly smaller than the degree of alignment of a with Z, resulting in a very small degree of three dimensional alignment. Comparison with Fig. 2 shows that these two strategies lead to a much lower degree of FF3DA than the orthogonally polarized two kick pulse approach detailed above.

In summary, we have explored three possible strategies for creating FF3DA, the most promising of which involves the use of two time-separated, orthogonally polarized kick laser pulses. This technique is completely general and readily applicable to a broad range of molecules. A significant advantage of this two pulse approach is that the electric field of the second pulse may be much higher than that of the minor axis of the ellipse when using an elliptically polarized field—for an elliptically polarized field, increasing the minor axis component of the field will serve to reduce the alignment of the most polarizable MF axis along the major axis of the ellipse. In the limit of circular polarization, the a axis will only be aligned to the plane of circular polarization, and no three dimensional alignment will be achieved. By arranging for the pulses to be time separated, we are able to avoid compromising the alignment of the first axis. The optimum width of the laser pulses will depend upon the rotational temperature and constants of the gas under study, and the temporal delay between the two laser pulses can be adjusted to coincide with the first revival of the figure axis of the molecule given by $t \sim 1/2(B_x + B_y)$. Future work will explore the use of other time separations and tailored sequence of orthogonally polarized laser pulses to further enhance this degree of FF3DA, as well as to the production of persistent FF3DA [29]. Additionally, we will explore the use of laser pulses with time varying polarization states, and the possible extension of this work to producing field-free three dimensional orientation.

J. G. U. acknowledges a Researcher Exchange Grant from the British Council and National Research Council of Canada.

*Electronic address: j.underwood@open.ac.uk

[1] B. Friedrich and D. Herschbach, Phys. Rev. Lett. **74**, 4623 (1995).
[2] H. Stapelfeldt and T. Seideman, Rev. Mod. Phys. **75**, 543 (2003).
[3] A. Stolow, Annu. Rev. Phys. Chem. **54**, 89 (2003).
[4] J. G. Underwood and K. L. Reid, J. Chem. Phys. **113**, 1067 (2000).
[5] Y. Suzuki *et al.*, Phys. Rev. Lett. **89**, 233002 (2002).
[6] R. Neutze *et al.*, Nature (London) **406**, 752 (2000).
[7] J. C. H. Spence and R. B. Doak, Phys. Rev. Lett. **92**, 198102 (2004).
[8] J. Miao *et al.*, Proc. Natl. Acad. Sci. U.S.A. **98**, 6641 (2001).
[9] J. C. Williamson *et al.*, Nature (London) **386**, 159 (1997).
[10] H. Niikura *et al.*, Nature (London) **417**, 917 (2002).
[11] H. Stapelfeldt *et al.*, Phys. Rev. Lett. **74**, 3780 (1995).
[12] S. Chelkowski *et al.*,Phys. Rev. Lett. **82**, 3416 (1999).
[13] J. Itatani *et al.*, Nature (London) **432**, 867 (2004).
[14] J. J. Larsen *et al.*, Phys. Rev. Lett. **85**, 2470 (2000).
[15] J. P. Heritage *et al.*, Phys. Rev. Lett. **34**, 1299 (1975).
[16] F. Rosca-Pruna and M. J. J. Vrakking, Phys. Rev. Lett. **87**, 153902 (2001).
[17] P. W. Dooley *et al.*, Phys. Rev. A **68**, 023406 (2003).
[18] E. Peronne *et al.*, Phys. Rev. Lett. **91**, 43003 (2003).
[19] M. Leibscher *et al.*, Phys. Rev. Lett. **90**, 213001 (2003).
[20] D. Sugny *et al.*, Phys. Rev. A **69**, 033402 (2004).
[21] M. Machholm and N. E. Henriksen, Phys. Rev. Lett. **87**, 193001 (2001).
[22] K. F. Lee *et al.*, J. Phys. B **37**, L43 (2004).
[23] C. Z. Bisgaard *et al.*, Phys. Rev. Lett. **92**, 173004 (2004).
[24] J. G. Underwood *et al.*, Phys. Rev. Lett. **90**, 223001 (2003).
[25] B. W. Shore, *The Theory of Coherent Atomic Excitation* (Wiley, New York, 1990), Vol. I and II.
[26] R. N. Zare, *Angular Momentum* (Wiley, New York, 1988).
[27] A. C. Kummel *et al.*, J. Chem. Phys. **88**, 6707 (1988).
[28] P. W. Joireman *et al.*, J. Chem. Phys. **96**, 4118 (1992).
[29] A. Matos-Abiague and J. Berakdar, Phys. Rev. A **68**, 063411 (2003).